

Supporting Information

Optimizing High-Efficiency Multiple Resonance Blue Delayed Fluorescent Emitters through Charge Transfer Excited State Tuning

Zhen Wang^a, Cheng Qu^a, Jie Liang^b, Xuming Zhuang^b, Yu Liu^{a,} and Yue Wang^a*

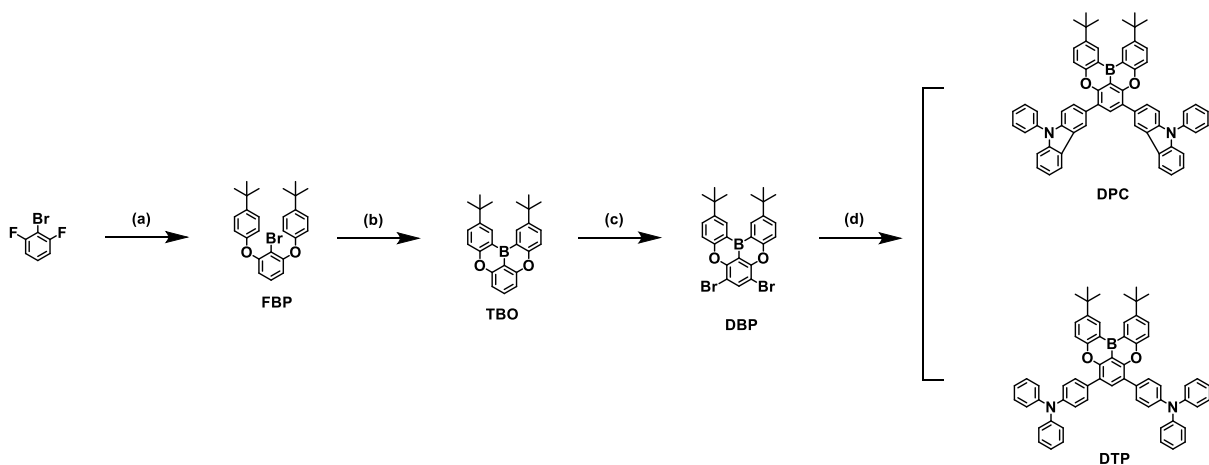
^aState Key Laboratory of Supramolecular Structure and Materials, College of Chemistry, Jilin University, Changchun 130012, P. R. China

^bJihua Laboratory, 28 Huandao South Road, Foshan, 528200, Guangdong Province, P. R. China

General Information: Thermo Fisher ITQ1100 GC/MS mass spectrometer was employed to measure the mass spectra. Flash EA 1112 spectrometer were used to perform the elemental analyses. Bruker AVANCE III 400 and 600 MHz spectrometers were selected to measure the ^1H and $^{13}\text{C}\{^1\text{H}\}$ NMR spectra, respectively, with tetramethylsilane (TMS) as the internal standard. Shimadzu RF-5301 PC spectrometer and Shimadzu UV-2550 spectrophotometer were adopted to record the PL emission spectra and UV-Vis absorption, respectively. The fluorescence and phosphorescent spectra taken at liquid nitrogen temperature (77 K) were recorded by Ocean Optics QE Pro with a 365 nm Ocean Optics LLS excitation source. Edinburgh FLS920 steady state fluorimeter equipping with an integrating sphere was employed to measure the absolute fluorescence quantum yields of both solutions and films. In the range of 25 to 800 °C, TA Q500 thermogravimeter was selected to perform the thermogravimetric analysis (TGA) of target molecules under nitrogen atmosphere at a heating rate of 10 K min⁻¹. BAS 100W Bioanalytical electrochemical work station was used to measure the electrochemical property with platinum disk as working electrode, platinum wire as auxiliary electrode, a porous glass wick Ag/Ag⁺ as pseudo reference electrode and ferrocene/ferrocenium as the internal standard. And 0.1 M solution of n-Bu₄NPF₆ which was the supporting electrolyte was utilized to measure the oxidation (in anhydrous CH₂Cl₂) or reduction (in anhydrous tetrahydrofuran) potentials at a scan rate of 100 mV s⁻¹. FLS920 fluorescence lifetime measurement system with 320 nm LED excitation source was selected to investigate the transient PL decay. The electrical characteristics of the OLEDs were determined using a Keithley 2400 source meter. The EL spectra and luminance of the OLED devices were recorded on a PR655 spectrometer. The device test data were all directly calculated by the software OSpectraM-OLED (version 2.1.6) supporting the corresponding instrument, without any processing or manual calculation.

Theoretical Calculations Method: We carried out the computational studies by using the density functional theory (DFT) in Gaussian 16 program package (revision A. 03)^[1]. All geometry optimizations of minima were conducted by using PBE0^[2] functional with Grimme's D3 dispersion correction, in conjunction with the Becke-Johnson (BJ) damping scheme^[3]. The 6-31G(d,p)^[4] as a basis set was adopted for all calculations. The vibrational frequencies analysis was performed at the same theoretical level to verify all stationary points as local minima (with no imaginary frequency). The vertical excitations were calculated (singlets and triplets) by time-dependent density functional theory (TD-DFT) method at the PBE0/6-31G(d,p) theoretical level based on the optimized ground-state structures. The geometry optimizations of the S₁ states were performed by TD-DFT method at the PBE0-D3(BJ)/6-31G(d,p) theoretical level using the optimized ground-state structures as starting coordinates. No symmetry constraint was used in any of the calculations. The SOC matrix elements were calculated by TD-DFT at the PBE0/6-31G(d,p) level using the ORCA program package (version 5.0.1)^[5]. Natural transition orbitals (NTOs)^[6] were analyzed by Multiwfn (version 3.8 dev)^[7]. All visualizations of geometric configurations, molecular orbitals, and directions of transition moments were performed by VMD (version 1.9.3)^[8].

Synthesis of Material: All reagents were purchased from *Energy Chemical Co.* immediately used without further purification. The Schlenk technology was strictly performed under nitrogen conditions in all reactions and the concrete synthesis procedures were showed below in detail. The final product was first purified by column chromatography, then temperature-gradient sublimation was utilized to further purify the target compound under high vacuum to obtain highly pure samples.



Scheme S1. Synthetic procedures of **DPC** and **DTP**.

Synthesis of FBP (a): A mixture of 2-Bromo-1,3-difluorobenzene (10.0 g, 51.8 mmol), 4-(tert-butyl)phenol (19.5 g, 129.5 mmol), and K_2CO_3 (17.8 g, 129.5 mmol) in N-methylpyrrolidinone (200 mL) was stirred at 170 °C for 22 hours. The reaction mixture was diluted with toluene and poured into H_2O . After separation of organic layer, aqueous layer was extracted with toluene twice. The organic layer was dried over anhydrous Na_2SO_4 and evaporated under reduced pressure, then purified by column chromatography over silica gel using petroleum ether as the eluent. The resulting residue was dried at 60 °C under vacuum to give the desired product (20.5 g) as a white solid. Yield: 87%. 1H NMR (600 MHz, Chloroform-*d*) δ /ppm: 7.40 – 7.36 (m, 4H), 7.13 (t, $J = 8.2$ Hz, 1H), 6.98 (d, $J = 8.8$ Hz, 4H), 6.68 (d, $J = 8.2$ Hz, 2H), 1.34 (s, 18H). $^{13}C\{^1H\}$ NMR (151 MHz, Chloroform-*d*) δ /ppm: 155.99, 154.24, 146.65, 128.15, 126.66, 118.21, 114.09, 107.24, 34.37, 31.51. ESI-MS (M): m/z : 453.31 $[M]^+$ (calcd: 452.14).

Synthesis of TBO (b): A solution of n-butyllithium in hexane (9.7 mL, 2.5 M, 24.3 mmol) was added slowly to a solution of FBP (10 g, 22.1 mmol) in anhydrous *tert*-butylbenzene (50 mL) at 0 °C under a nitrogen atmosphere. After 30 minutes, the mixture was stirred at room temperature for 1 h. Then boron tribromide (3.2 mL, 33.2 mmol) was added slowly at 0 °C. After

20 minutes, the mixture was stirred at room temperature for 1 hour. Then *N,N*-diisopropylethylamine (7.3 mL, 44.2 mmol) was added at 0 °C and then the reaction mixture was allowed to room temperature. The reaction mixture was stirred at room temperature for 30 minutes, and 150 °C for 26 h, and then cooled to room temperature. After the addition of saturated brine to the reaction mixture, the aqueous layer was separated and extracted with 200 mL dichloromethane. After the solvent was removed in vacuo, the crude product was purified by column chromatography (petroleum ether) to obtain the desired compound (5.6 g) as a white solid Yield: 66%. ¹H NMR (600 MHz, Chloroform-*d*), δ/ppm: ¹H NMR (600 MHz, Chloroform-*d*) δ 8.75 (d, J = 2.5 Hz, 2H), 7.94 – 7.65 (m, 3H), 7.49 (d, J = 8.7 Hz, 2H), 7.33 – 6.93 (m, 2H), 1.49 (s, 18H). ¹³C{¹H} NMR (151 MHz, Chloroform-*d*) δ/ppm: 158.66, 157.57, 144.93, 134.33, 131.46, 130.25, 121.72, 118.00, 108.23, 34.55, 31.57. ESI-MS (M): m/z: 382.33 [M]⁺ (calcd: 382.21).

Synthesis of DBP (c): TBO (1 g, 2.62 mmol) and N-bromosuccinimide (1.16 g, 6.54 mmol), were added with dry THF (20 mL) at 0 °C for 2 h. Then the mixture was heated to 25 °C slowly and stirred overnight. Afterward, the reaction mixture was extracted with dichloromethane and water, and the combined organic layer was condensed in vacuum, and then the crude product was further purified by column chromatography to afford a white solid (1.1 g). Yield: 77%. ¹H NMR (600 MHz, Chloroform-*d*), δ/ppm: 8.75 (d, J = 2.5 Hz, 2H), 8.16 (s, 1H), 7.83 (dd, J = 8.8, 2.4 Hz, 2H), 7.60 (d, J = 8.7 Hz, 2H), 1.50 (d, J = 1.1 Hz, 18H). ¹³C{¹H} NMR (151 MHz, Chloroform-*d*) δ/ppm: δ 158.28, 152.52, 145.93, 139.51, 132.16, 130.15, 118.30, 101.17, 67.99, 34.66, 31.52, 25.62. ESI-MS (M): m/z: 540.11 [M]⁺ (calcd: 540.03).

Synthesis of DPC (d): DBP (0.6 g, 1.11 mmol), 9-Phenyl-9H-carbazol-3-ylboronic acid (1.0 g, 3.48 mmol), potassium carbonate (461 mg, 3.34 mmol), deionized water (2 mL), ethanol (2 mL)

and toluene (30 mL) were added to a 100 mL two-necked flask. The mixture was bubbled with nitrogen for further 10 minutes, and tetrakis(triphenylphosphine)palladium(0) (66.5 mg, 0.057 mmol) was added under a high flow of nitrogen. Then the mixture was heated to reflux and stirred overnight. After cooling to room temperature, the reaction mixture was extracted with dichloromethane and water, and the combined organic layer was condensed in vacuum, and then the crude product was further purified by column chromatography to afford a light yellowish green solid (824 mg). Yield: 86%. ^1H NMR (400 MHz, Chloroform-*d*), δ /ppm: 8.84 (s, 2H), 8.62 (s, 1H), 8.28 – 8.16 (m, 3H), 7.93 (d, $J = 8.6$ Hz, 2H), 7.76 (d, $J = 11.1$ Hz, 2H), 7.67 (d, $J = 6.0$ Hz, 9H), 7.59 (d, $J = 8.2$ Hz, 2H), 7.53 – 7.43 (m, 8H), 7.32 (t, $J = 6.9$ Hz, 2H), 1.51 (s, 18H). $^{13}\text{C}\{^1\text{H}\}$ NMR (151 MHz, Chloroform-*d*) δ /ppm: 155.99, 154.24, 146.65, 128.15, 126.66, 118.21, 114.09, 107.24, 34.37, 31.51. ESI-MS (M): m/z : 864.05 $[\text{M}]^+$ (calcd: 864.39). Anal. Calcd for $\text{C}_{56}\text{H}_{55}\text{BN}_4$: C, 86.10; H, 5.59; N, 3.27. Found: C, 86.29; H, 5.65; N, 3.27.

Synthesis of DTP (d): A similar procedure like synthesizing **DPC** was carried out except replacing compound 9-Phenyl-9H-carbazol-3-ylboronic acid with compound 4-(Diphenylamino)phenylboronic acid (0.96 g, 3.34 mmol), resulting in a yellow-green solid (768 mg). Yield: 80%. ^1H NMR (400 MHz, Chloroform-*d*), δ /ppm: 8.79 (s, 2H), 7.98 (s, 1H), 7.76 (d, $J = 6.5$ Hz, 2H), 7.71 (d, $J = 8.6$ Hz, 4H), 7.46 (d, $J = 8.8$ Hz, 2H), 7.30 (t, $J = 7.8$ Hz, 8H), 7.21 (d, $J = 7.6$ Hz, 12H), 7.05 (t, $J = 7.2$ Hz, 4H), 1.49 (s, 18H). $^{13}\text{C}\{^1\text{H}\}$ NMR (151 MHz, Chloroform-*d*) δ /ppm: 155.99, 154.24, 146.65, 128.15, 126.66, 118.21, 114.09, 107.24, 34.37, 31.51. ESI-MS (M): m/z : 868.92 $[\text{M}]^+$ (calcd: 868.42). Anal. Calcd for $\text{C}_{56}\text{H}_{55}\text{BN}_4$: C, 85.70; H, 6.15; N, 3.22.; N, 3.22; Found: C, 85.81; H, 6.11; N, 3.28.

Device Fabrication and Measurements: Before device fabrication, the indium tin oxide (ITO) glass substrates with a sheet resistance of 15Ω per square were treated with plasma for 5 min, after cleaning with optical detergents, deionized water, acetone and isopropanol successively. Then they were transferred to a vacuum chamber in a nitrogen-filled glove box. Under high vacuum ($< 5 \times 10^{-5}$ Pa), the organic materials were deposited onto the ITO glass substrates at a rate of 1 \AA s^{-1} . After finishing the deposition of organic layers, ITO glass substrates were patterned by a shadow mask with an array of $2.0 \text{ mm} \times 2.5 \text{ mm}$ openings. Then LiF and Al were successively deposited at a rate of 0.1 \AA s^{-1} and 5 \AA s^{-1} , respectively. The EL spectra, CIE coordinates and luminance intensities of the OLEDs were recorded by Photo Research PR655, simultaneously, the current density (J) and driving voltage (V) were recorded by Keithley 2400. By assuming a Lambertian distribution, the EQE was estimated based on the brightness, electroluminescence spectrum, and current density.

Calculation Formulas for the Photophysical Parameters: The calculation formulas for the rate constants of fluorescent (k_F), internal conversion (k_{IC}), intersystem crossing (k_{ISC}), TADF (k_{TADF}) and reverse intersystem crossing (k_{RISC}) are expressed as following list:^[9-12]

$$k_F = \Phi_F / \tau_F \quad (\text{S1})$$

$$\Phi_{PL} = k_F / (k_F + k_{IC}) \quad (\text{S2})$$

$$\Phi_F = k_F / (k_F + k_{IC} + k_{ISC}) \quad (\text{S3})$$

$$\Phi_{ISC} = k_{ISC} / (k_F + k_{IC} + k_{ISC}) \quad (\text{S4})$$

$$k_{TADF} = \Phi_{TADF} / (\Phi_{ISC} \tau_{TADF}) \quad (\text{S5})$$

$$k_{RISC} = k_F k_{TADF} \Phi_{TADF} / (k_{ISC} \Phi_F) \quad (\text{S6})$$

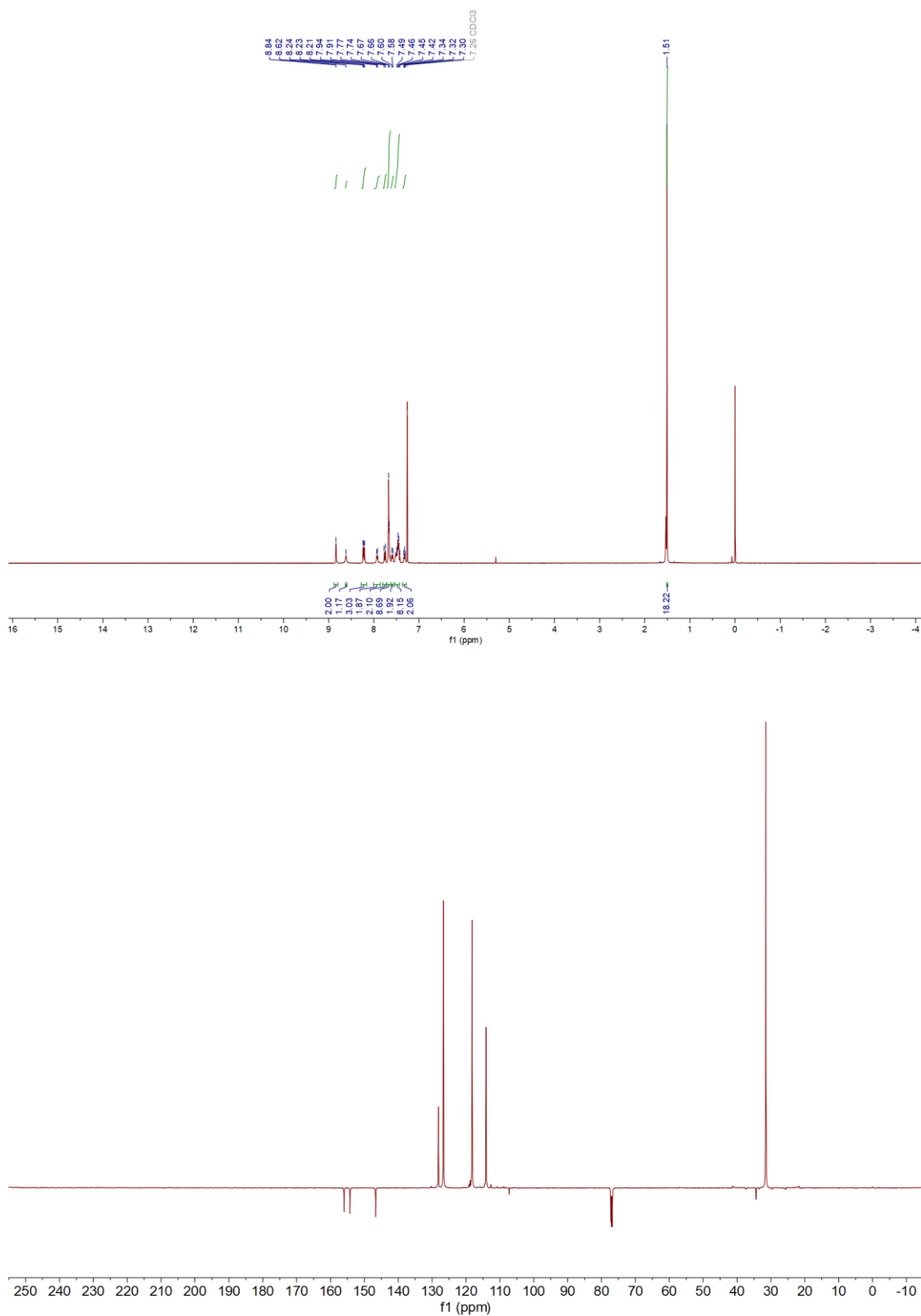


Figure S1. ^1H NMR spectrum (400 MHz, CDCl_3) (top) and $^{13}\text{C}\{^1\text{H}\}$ NMR spectrum (151 MHz, CDCl_3) (bottom) of DPC.

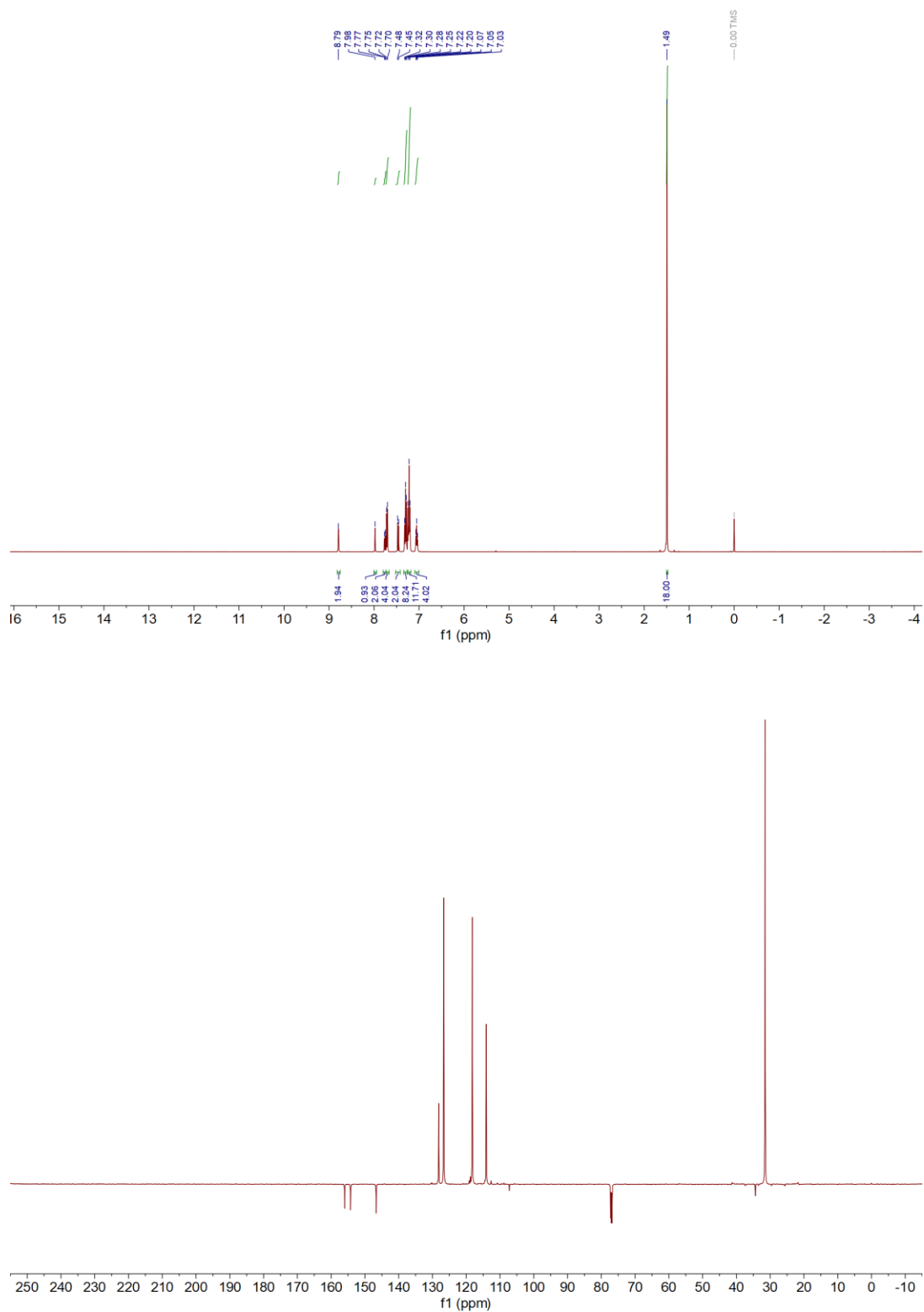


Figure S2. ^1H NMR spectrum (400 MHz, CDCl_3) (top) and $^{13}\text{C}\{^1\text{H}\}$ NMR spectrum (151 MHz, CDCl_3) (bottom) of DTP.

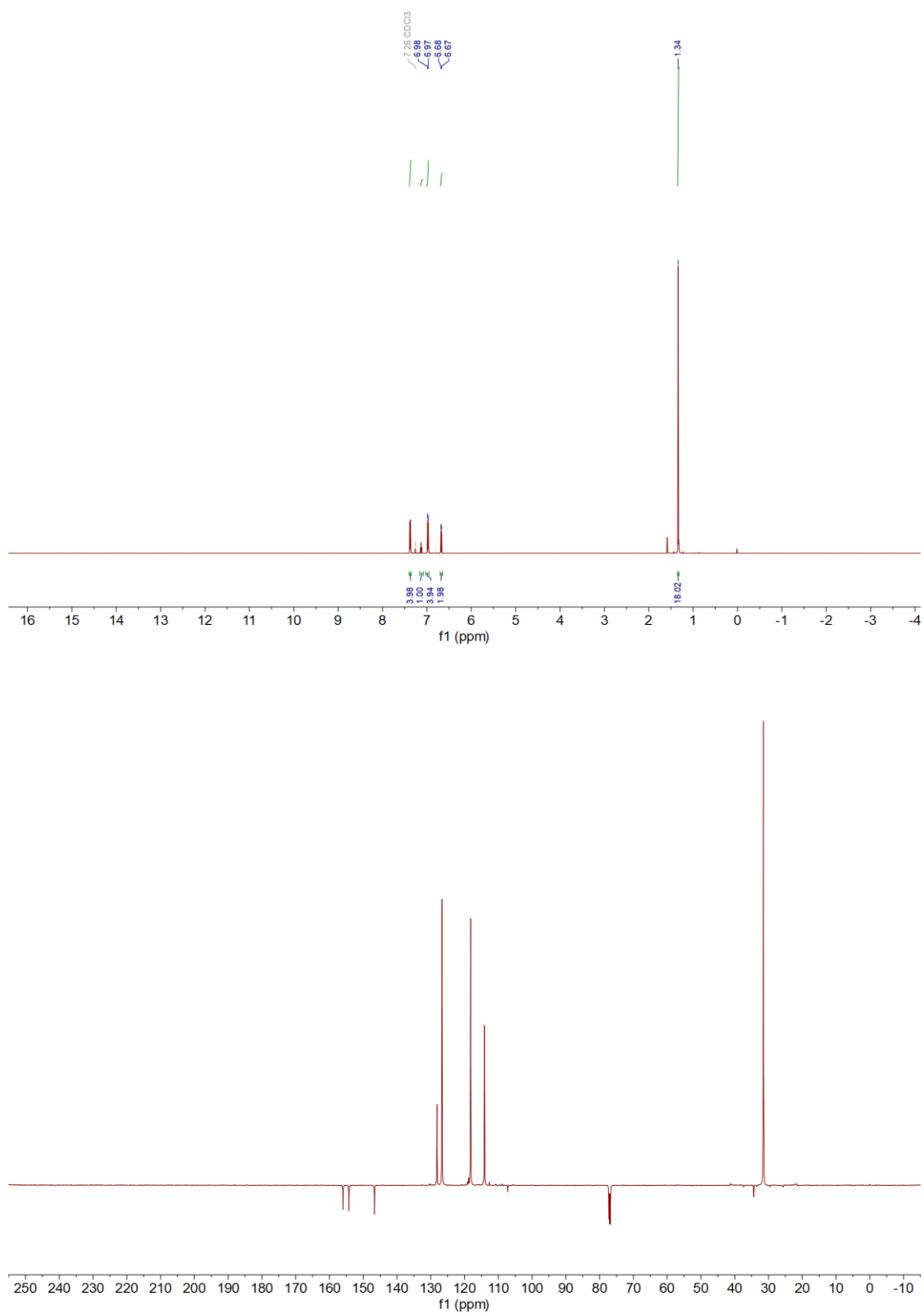


Figure S3. ^1H NMR spectrum (500 MHz, CDCl_3) (top) and $^{13}\text{C}\{^1\text{H}\}$ NMR spectrum (151 MHz, CDCl_3) (bottom) of **FBP**.

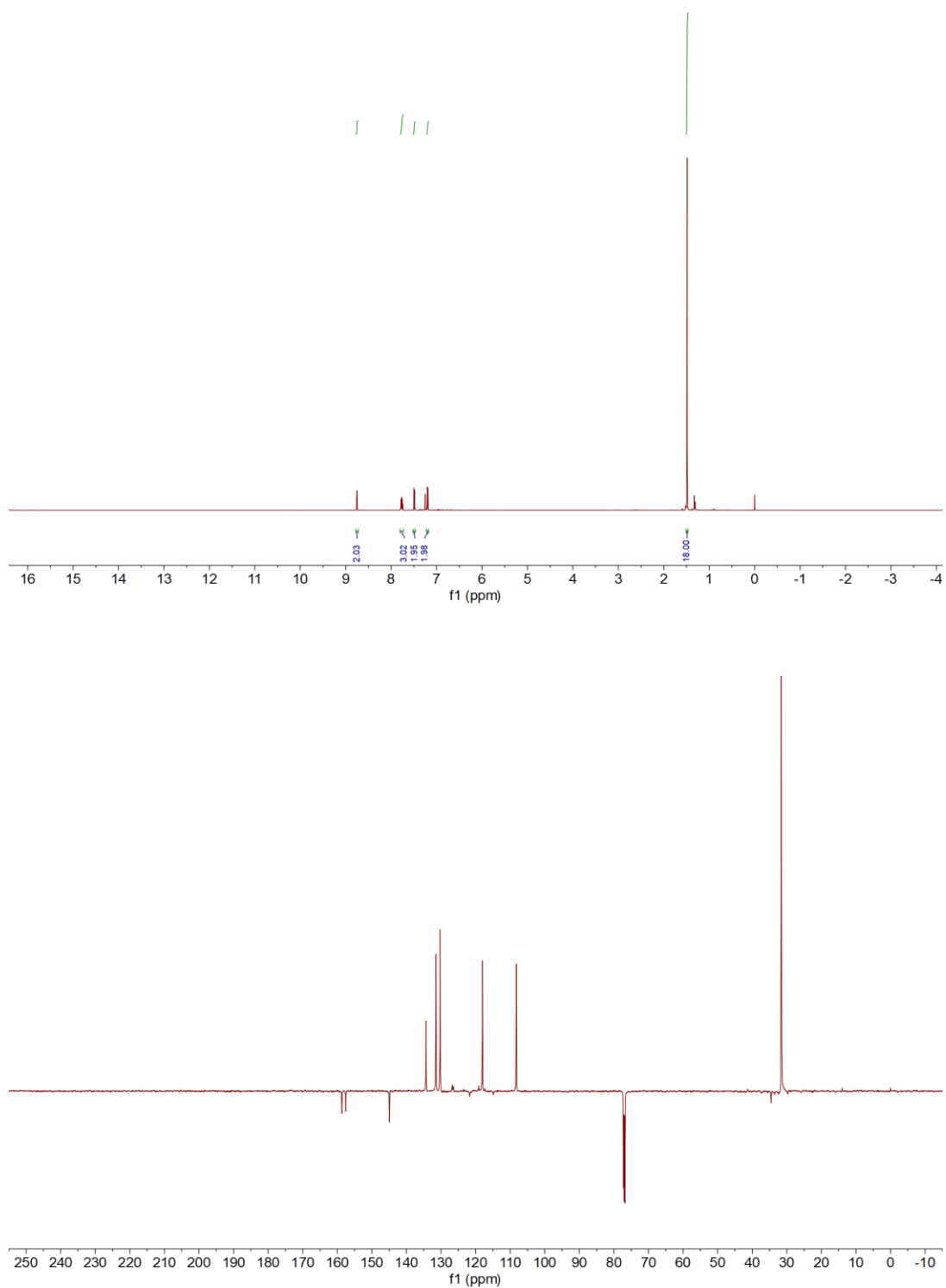


Figure S4. ^1H NMR spectrum (500 MHz, CDCl_3) (top) and $^{13}\text{C}\{^1\text{H}\}$ NMR spectrum (151 MHz, CDCl_3) (bottom) of **TBO**.

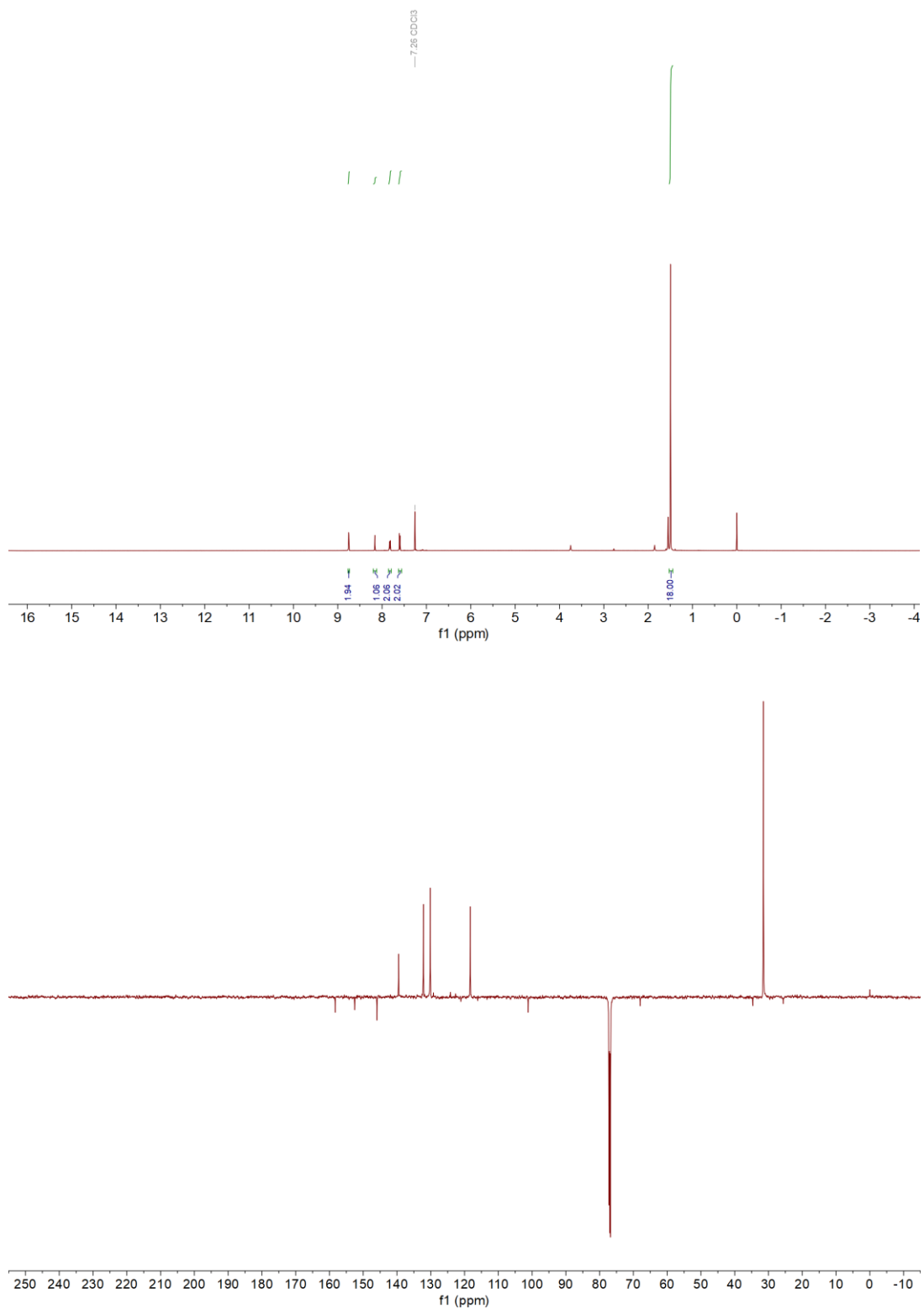


Figure S5. ^1H NMR spectrum (500 MHz, CDCl_3) (top) and $^{13}\text{C}\{^1\text{H}\}$ NMR spectrum (151 MHz, CDCl_3) (bottom) of **DBP**.

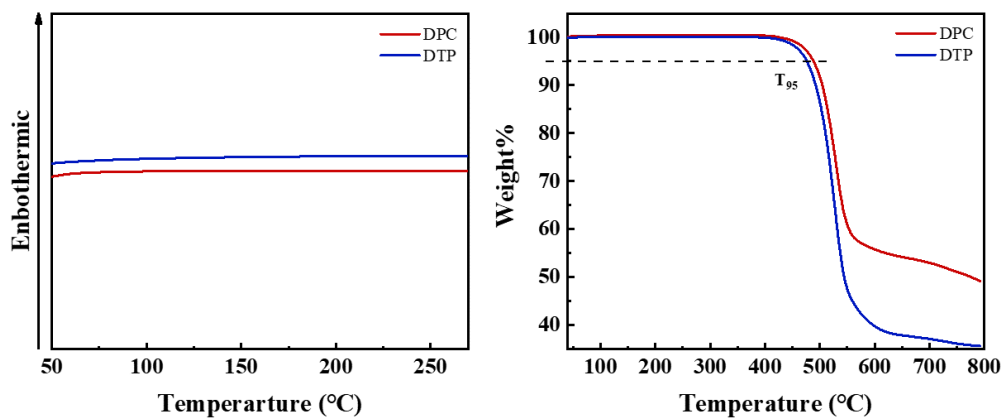


Figure S6. TGA and DSC curves of **DPC** and **DTP**.

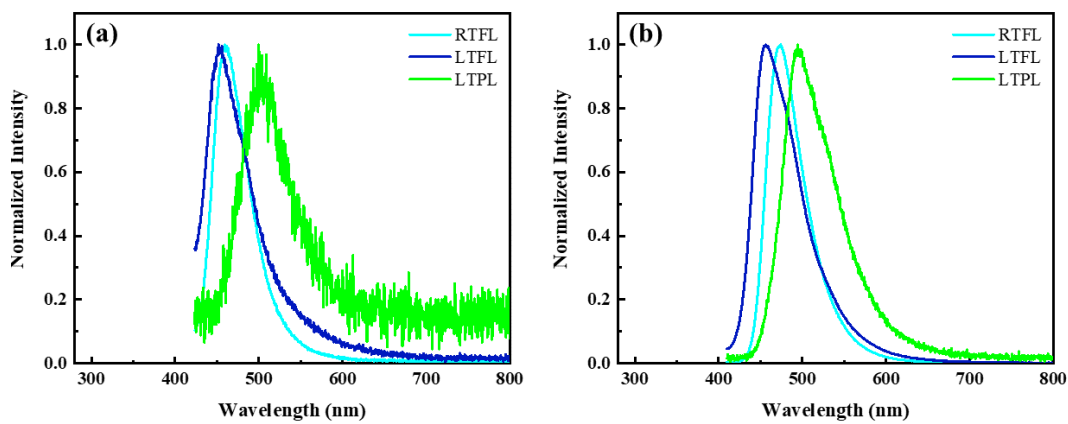


Figure S7. The normalized fluorescence (RTFL and LTFL) and phosphorescence spectra (LTPL) of **DPC** (a) and **DTP** (b) measured in toluene solutions (1×10^{-5} M) at room temperature and 77K

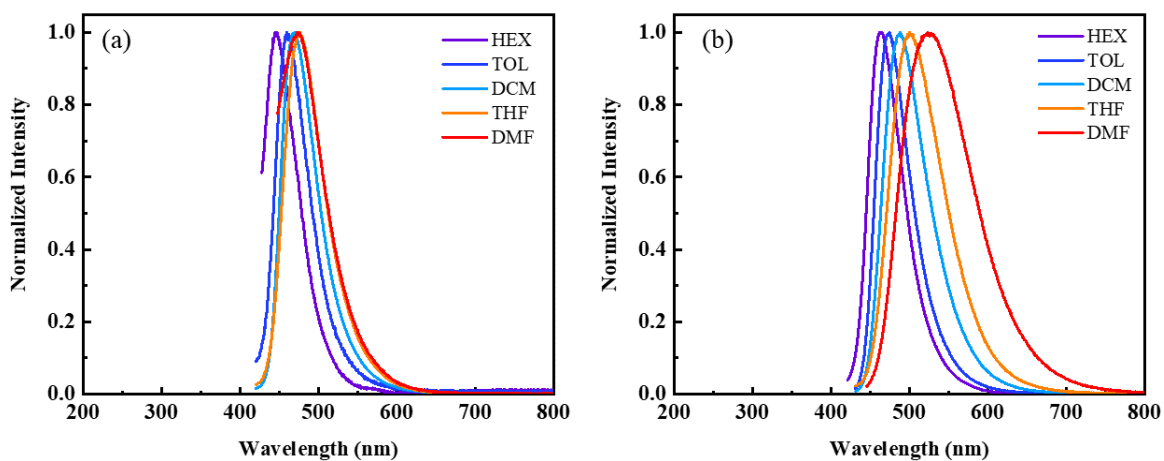


Figure S8. The normalized photoluminescence (c, d) spectra of **DPC** and **DTP** measured at room temperature with various solvents

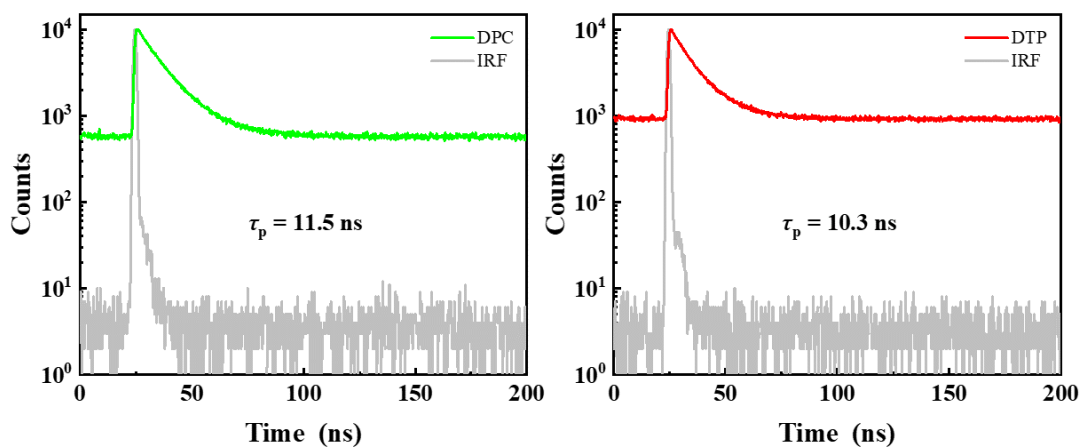


Figure S9. Room-temperature fluorescence decay curves of 6 wt% doped films of **DPC** and **DTP**

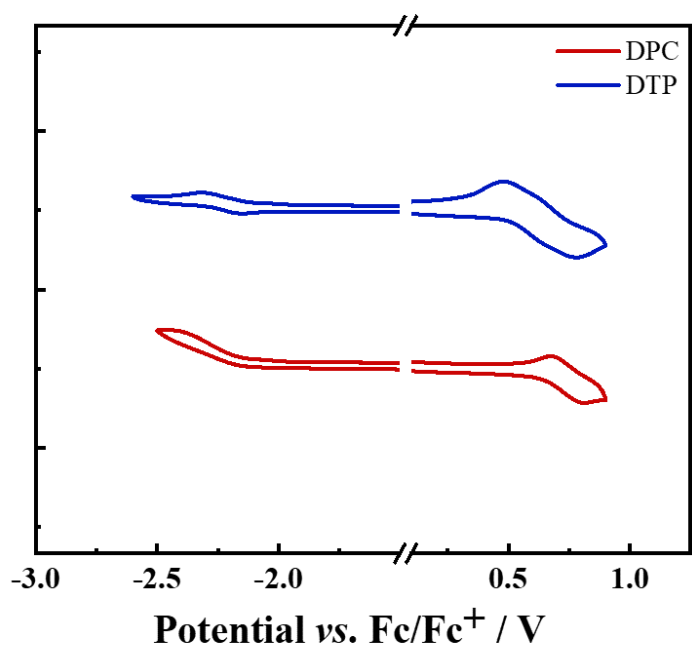


Figure S10. CV curves of **DPC** and **DTP**.

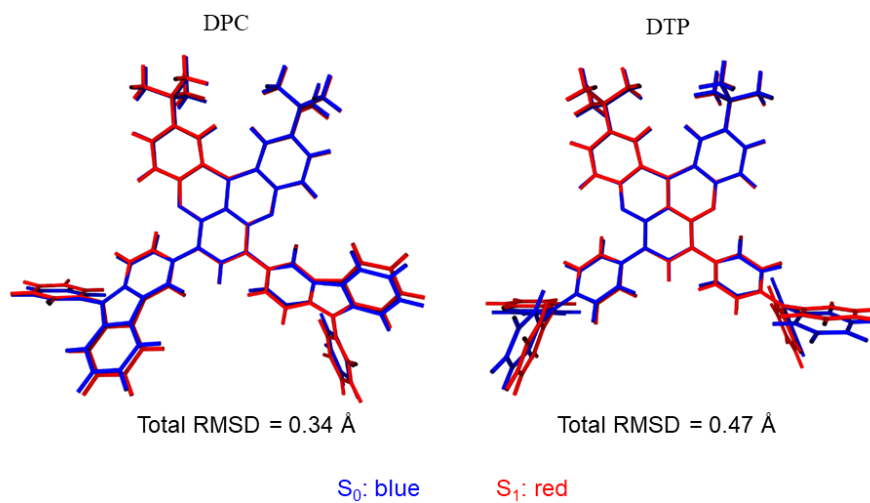


Figure S11. Geometry comparisons between the optimized S₀ and S₁ states of of **DPC** and **DTP** (RMSD)

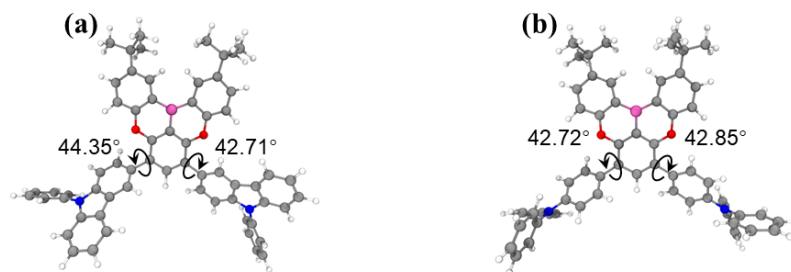
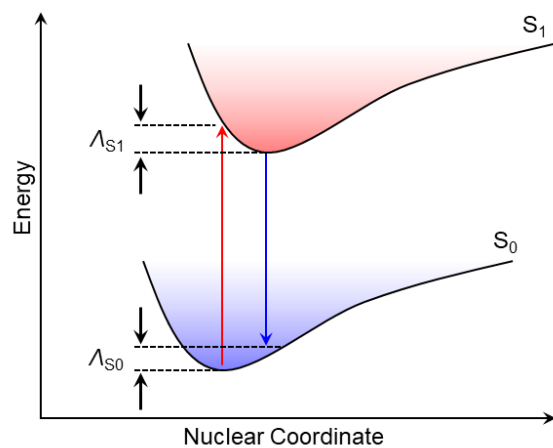


Figure S12. The dihedral angles between the donor and the B-substituted phenyl-ring of **DPC** (a) and **DTP** (b)



	DPC	DTP
Λ_{S1} / eV	0.20	0.56
Λ_{S0} / eV	0.23	0.20
Λ_{total} / eV	0.43	0.76

Figure S13. The reorganization energies (Λ) of **DPC** (a) and **DTP** (b)

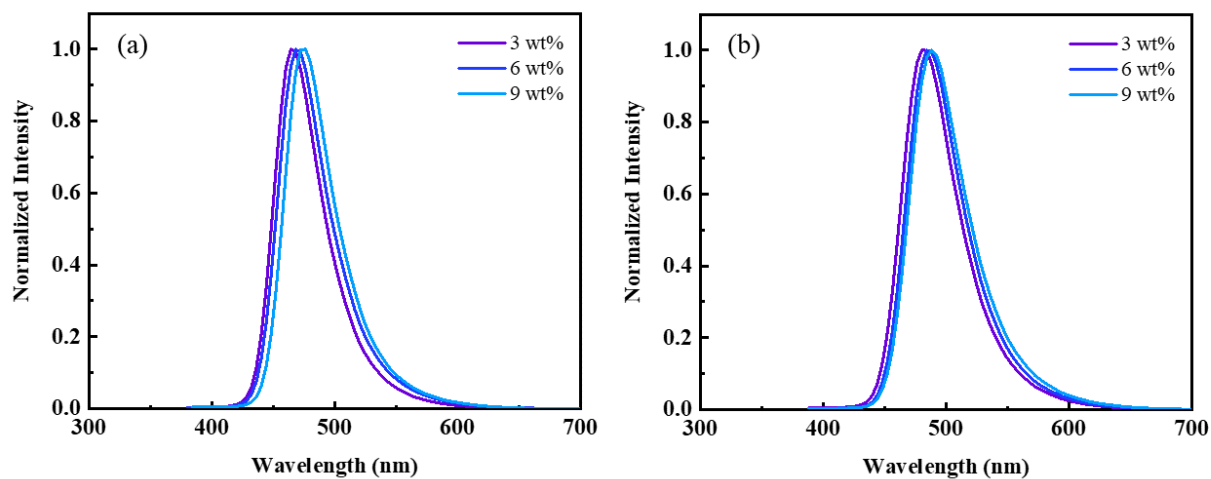


Figure S14. The EL spectra of DPC (a) and DTP(b)-based OLEDs with 3 wt% doping in BCPO at the brightness of 100 cd/m²

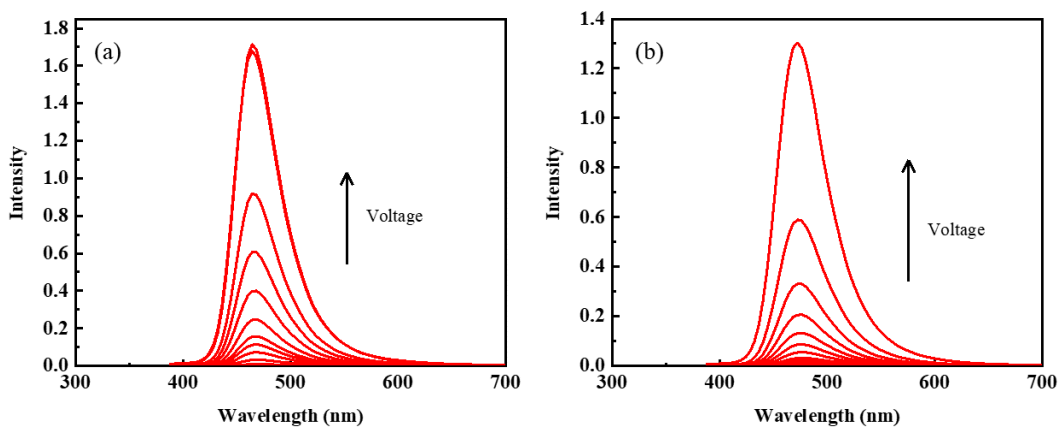


Figure S15. Original voltage-dependent EL spectra operated of **DPC** (a) and **DTP** (b) devices (6 wt% doping concentration)

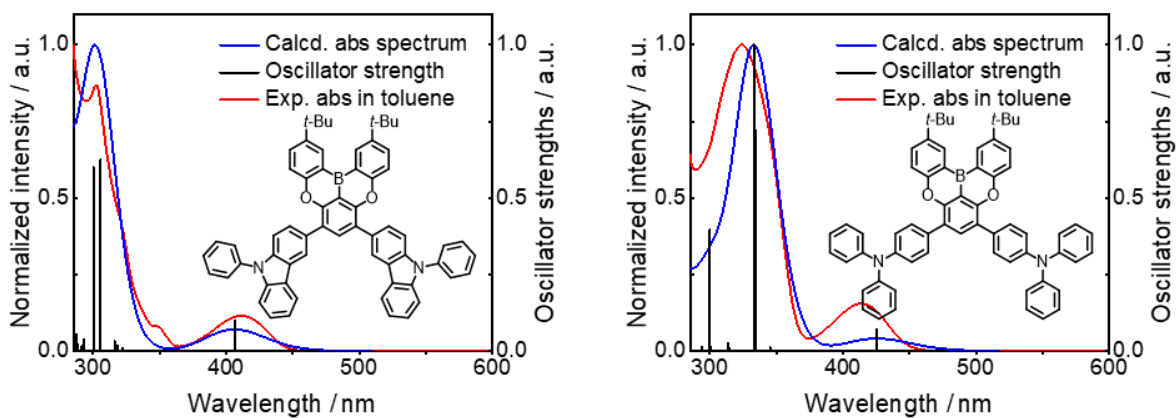


Figure S16. Comparison between the calculated and experimental absorption spectra of **DPC** (a) and **DTP** (b)

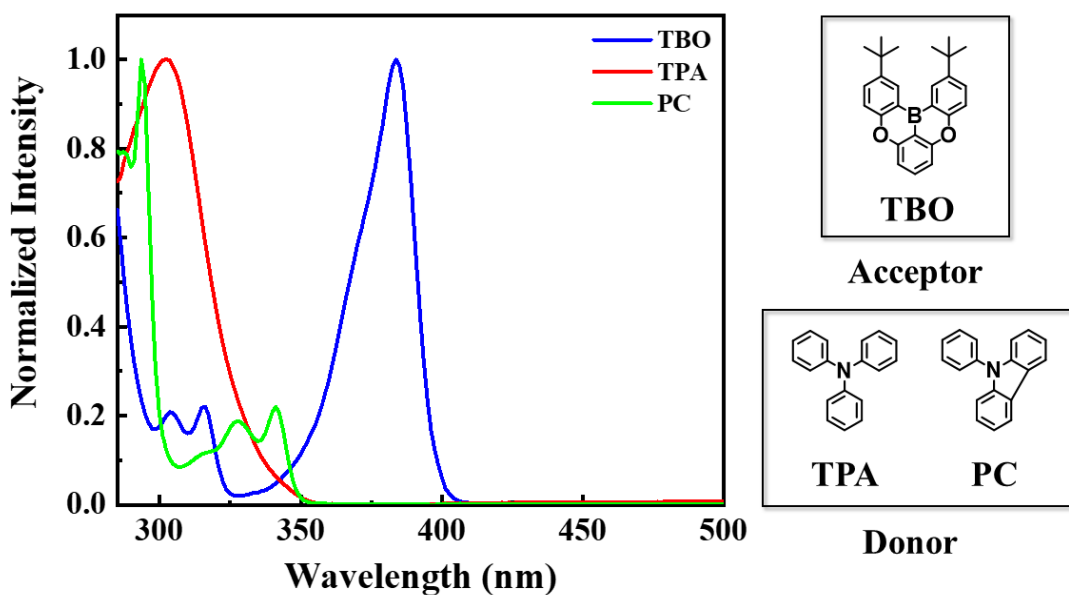


Figure S17. Room-temperature Ultraviolet–visible (UV–vis) absorption spectra and molecular structures of **TBO** (the acceptor of **DTP** and **DPC**), **TPA** (the donor of **DTP**) and **PC** (the donor of **DPC**) measured in toluene solutions (10^{-5} M)

Table S1. Summary of performance for high-efficiency narrowband TADF emitters based on oxygen-bridged boron.

Emitter	$\lambda_{\text{FL}}/\text{FWHM}^{\text{a}}$ [nm]	$\lambda_{\text{EL}}/\text{FWHM}^{\text{b}}$ [nm]	$\text{CIE}_{(x,y)}$	$\text{EQE}_{\text{ma}}^{\text{c}}$ [%]	$\text{PE}_{\text{max}}^{\text{d}}$ [lm W ⁻¹]	Ref.
DPC	458/44	464/47	(0.14, 0.15)	38.6	59.6	This work
DTP	470/50	476/53	(0.14, 0.25)	28.1	58.6	This work
TDBA-DI	456/55	—/65	(0.15, 0.28)	38.2	57.2	13
TDBA-Ac	456/50	—/55	(0.14, 0.15)	25.7	25.4	13
DBA-BFICz	446/—	476/64	(0.15, 0.24)	33.2	—	14
3CzTB	433/—	470/—	(0.14, 0.19)	29.1	—	15
M3CzB	445/—	478/—	(0.14, 0.26)	30.7	—	15
5TBO	457/47	484/57	(0.12, 0.27)	26.2	—	16
OBO-II	450/53	468/59	(0.14, 0.17)	33.8	48.6	17
DBA-DmICz	448/58	485/48	(0.16, 0.34)	31.6	—	18
DBA-DTMCz	455/53	479/58	(0.14, 0.27)	37.0	—	18
TDBA-SBA	450/—	467/55	(0.13, 0.21)	29.2	30.8	19
1BOICz	527/85	534/101	(0.38, 0.56)	34.6	95.5	20
2BOICz	518/83	528/91	(0.38, 0.55)	40.4	122	20
PzTDBA	599/—	576/—	(0.49, 0.50)	30.3	—	21

^a Peak wavelength of fluorescence spectrum and full-width at half-maximum in dilute solution. ^b

Peak wavelength of electroluminescence spectrum and full-width at half-maximum. ^c Maximum

external quantum efficiency ^d Maximum power efficiency.

References

- (1) Gaussian 16, Revision A.03, M. J. Frisch, G. W. Trucks, H. B. Schlegel, G. E. Scuseria, M. A. Robb, J. R. Cheeseman, G. Scalmani, V. Barone, G. A. Petersson, H. Nakatsuji, X. Li, M. Caricato, A. V. Marenich, J. Bloino, B. G. Janesko, R. Gomperts, B. Mennucci, H. P. Hratchian, J. V. Ortiz, A. F. Izmaylov, J. L. Sonnenberg, D. Williams-Young, F. Ding, F. Lipparini, F. Egidi, J. Goings, B. Peng, A. Petrone, T. Henderson, D. Ranasinghe, V. G. Zakrzewski, J. Gao, N. Rega, G. Zheng, W. Liang, M. Hada, M. Ehara, K. Toyota, R. Fukuda, J. Hasegawa, M. Ishida, T. Nakajima, Y. Honda, O. Kitao, H. Nakai, T. Vreven, K. Throssell, J. A. Montgomery, Jr., J. E.

Peralta, F. Ogliaro, M. J. Bearpark, J. J. Heyd, E. N. Brothers, K. N. Kudin, V. N. Staroverov, T. A. Keith, R. Kobayashi, J. Normand, K. Raghavachari, A. P. Rendell, J. C. Burant, S. S. Iyengar, J. Tomasi, M. Cossi, J. M. Millam, M. Klene, C. Adamo, R. Cammi, J. W. Ochterski, R. L. Martin, K. Morokuma, O. Farkas, J. B. Foresman, and D. J. Fox, Gaussian, Inc., Wallingford CT, **2016**.

(2) C. Adamo, V. Barone, *J. Chem. Phys.* **1999**, *110*, 6158.

(3) a) S. Grimme, J. Antony, S. Ehrlich, H. Krieg, *J. Chem. Phys.* **2010**, *132*, 154104. b) S. Grimme, S. Ehrlich, L. Goerigk, *J. Comput. Chem.* **2011**, *32*, 1456.

(4) P. C. Hariharan, J. A. Pople, *Theoret. Chim. Acta* **1973**, *28*, 213.

(5) a) F. Neese, *WIREs Comput. Mol. Sci.* **2012**, *2*, 73; b) F. Neese, *WIREs Comput. Mol. Sci.* **2018**, *8*, e1327; c) F. Neese, F. Wennmohs, U. Becker, C. Riplinger, *J. Chem. Phys.* **2020**, *152*, 224108.

(6) R. L. Martin, *J. Chem. Phys.* **2003**, *118*, 4775.

(7) T. Lu, F. Chen, *J. Comput. Chem.* **2012**, *33*, 580.

(8) W. Humphrey, A. Dalke, K. Schulten, *J. Molec. Graphics* **1996**, *14*, 33.

(9) Q. Zhang, H. Kuwabara, W. J. Potscavage, S. Huang, Y. Hatae, T. Shibata, C. Adachi, *J. Am. Chem. Soc.* **2014**, *136*, 18070–18081.

(10) Q. Zhang, B. Li, S. Huang, H. Nomura, H. Tanaka, C. Adachi, *Nat. Photonics* **2014**, *8*, 326–332.

- (11) S. Oda, W. Kumano, T. Hama, R. Kawasumi, K. Yoshiura, T. Hatakeyama, *Angew. Chem. Int. Ed.* **2021**, *60*, 2882–2886.
- (12) T. Hatakeyama, K. Shiren, K. Nakajima, S. Nomura, S. Nakatsuka, K. Kinoshita, J. Ni, Y. Ono, T. Ikuta, *Adv. Mater.* **2016**, *28*, 2777–2781.
- (13) D. H. Ahn, S. W. Kim, H. Lee, I. J. Ko, D. Karthik, J. Y. Lee, J. H. Kwon, *Nat. Photonics* **2019**, *13*, 540–546.
- (14) R. Braveenth, H. Lee, J. D. Park, K. J. Yang, S. J. Hwang, K. R. Naveen, R. Lampande, J. H. Kwon, *Adv. Funct. Mater.* **2021**, *31*, 2105805.
- (15) D. Karthik, D. H. Ahn, J. H. Ryu, H. Lee, J. H. Maeng, J. Y. Lee, J. H. Kwon, *J. Mater. Chem. C* **2020**, *8*, 2272–2279.
- (16) X. Y. Meng, Z. Q. Feng, Y. J. Yu, L. S. Liao, Z. Q. Jiang, *Molecules* **2022**, *27*, 4048.
- (17) I. S. Park, H. Min, J. U. Kim, T. Yasuda, *Adv. Opt. Mater.* **2021**, *9*, 2101282.
- (18) H. Lee, R. Braveenth, S. Muruganatham, C. Y. Jeon, H. S. Lee, J. H. Kwon, *Nat. Commun.* **2023**, *14*, 419.
- (19) T. Hua, Y. C. Liu, C. W. Huang, N. Li, C. Zhou, Z. Huang, X. Cao, C. C. Wu, C. Yang, *Chem. Eng. J.* **2022**, *433*, 133598.
- (20) G. Meng, H. Dai, Q. Wang, J. Zhou, T. Fan, X. Zeng, X. Wang, Y. Zhang, D. Yang, D. Ma, D. Zhang, L. Duan, *Nat. Commun.* **2023**, *14*, 2394.
- (21) D. Karthik, Y. H. Jung, H. Lee, S. Hwang, B.-M. Seo, J.-Y. Kim, C. W. Han, J. H. Kwon, *Adv. Mater.* **2021**, *33*, 2007724.